Characteristics of Negative Lightning Return Strokes in a Tropical and Non-Tropical Region—A Comparative Perspective

Faranadia Abdul Haris[1,2]*, Mohd Zainal Abidin Ab. Kadir[1], Jasronita Jasni[1], Dalina Johari[2] and Muhammad Haziq Muhammad Sabri[3]

[1]*Advanced Lightning, Power and Energy Research (ALPER), Faculty of Engineering, Universiti Putra Malaysia,43400 UPM, Serdang, Selangor, Malaysia*
[2]*School of Electrical, College of Engineering, Universiti Teknologi MARA Shah Alam, 40450 UiTM, Selangor, Malaysia*
[3]*College of Engineering, Universiti Tenaga Nasional, 43000 UNITEN, Kajang, Malaysia*

ABSTRACT

Lightning is a naturally occurring phenomenon that involves a sudden electrostatic discharge caused by an imbalance between electrically charged cloud regions. Although lightning is visibly amazing, its impact can be dangerous and damaging, which many studies have carried out lightning-generated electric field measurements to assess the electrical discharge features. This study conducted the lightning-generated electric field measurement on the College of Engineering building rooftop at UNITEN from August 2019 to March 2020. A total of 115 negative lightning return strokes waveforms were recorded using a parallel plate antenna. A comparison was made between the data measured in the tropical and non-tropical regions, such as UTM, UPM, Sweden, USA, and Germany, in terms of the characteristic, mainly on the negative return strokes parameters. It was observed that data measured in the same region, either tropical or non-tropical, were consistent or almost similar. On the contrary, the results indicated a significant difference between these two regions on the negative return strokes parameters characteristics. The zero-to-peak and fast transition 10–90% rise time, as well as width dE/dt pulse at half peak value in the tropical region, were observed higher than the non-tropical region. Meanwhile, the zero-crossing time and slow front amplitude relative to the peak in the non-tropical region were averagely longer as compared to the tropical region. Therefore, dissimilarities in

Faranadia Abdul Haris, Mohd Zainal Abidin Ab. Kadir, Jasronita Jasni, Dalina Johari and Muhammad Haziq Muhammad Sabri

the characteristics of negative return stroke parameters could be attributed to the variation in the meteorological conditions, geographical locations, and climatic affection.

Keywords: Electric field, lightning, negative return stroke, non-tropical, parallel-plate antenna, tropical

INTRODUCTION

Lightning is a natural phenomenon that involves a sudden electrostatic discharge commonly during thunderstorm days, which can occur either between electrically charged regions of the cloud (intra-cloud lightning), between clouds (cloud-to-cloud lightning), or between a cloud and the ground (cloud-to-ground lightning) (Shivalli, 2016; Arshad, 2017; Nag & Rakov, 2014). The high current produced by a lightning flash of up to tens of kA can harm humans and damage electronic and electrical systems (Sokol & Popová, 2021; Wang et al., 2021). In addition, the brightness and intensity of lightning flash against the cloud create otherworldly nature phenomena. Lightning can be described, according to Master and Uman (1984), as a transient, high-current (typically tens of kilo amperes) electric discharge in the air whose length is measured in kilometres (Rakov & Uman, 2003). About 90% or more of global cloud-to-ground lightning is accounted for by negative lightning, i.e., negative charge is effectively transported to the ground, where the initial process begins in the cloud and develops in the downward direction (Dwyer & Uman, 2014; Rakov, 2013).

Generally, a lightning phenomenon can be categorised into two types, namely ground flashes (i.e. the lightning strike makes direct contact with the ground) and cloud flashes (i.e. the lightning strike does not reach out to the ground part (Cooray & Fernando, 2009). The ground flash can be further subdivided into downward ground flash, initiated from the cloud and upward ground flash, actuated from a tall structure (Cooray & Fernando, 2009). Each of these ground flashes consists of positive and negative types. Meanwhile, the cloud flashes occur either within a thundercloud, between thunderclouds or between a thundercloud with clear air. Cloud flashes account for the majority of all lightning discharges (Cooray, 2015; Dwyer & Uman, 2014). Nevertheless, the ground flashes of lightning might be the most damaging as they could cause property damages, start fires, and cause injuries, even fatalities to people. The return stroke in a negative cloud-to-ground lightning discharge is thought to be preceded by the initial or preliminary breakdown, which can be defined as the in-cloud process that initiates or leads to the initiation of the downward-moving stepped leader (Cooray, 1997).

The overall effect of lightning is called a flash, consisting of several strokes. The lightning strike can be defined as a lightning flash attaching to a structure where the electric fields in the thundercloud are typically 100–200 kV/m and can be as high as 400 kV/m. The ground flash mechanism involves many physical processes, such as preliminary breakdown, stepped leaders, connecting leaders, and return strokes (Ahmad et al., 2010). The most common downward ground flash is a negative ground flash initiated by a lower negative

charge region from the thundercloud to the ground. The preliminary breakdown process refers to an electrical breakdown initiation inside the thundercloud, consisting of multitudes of discharges that lead to a leader's development that propagates in a stepped structure towards the ground. The stepped leader constructs branches as it propagates, which induces opposite polarity charges on objects projecting above the earth's surface as it approaches the ground part. According to the basic electrostatic force theory, when two objects carry a different charge, they will attract each other. Similarly, the induced charges attempt to join the downward-moving stepped leader by forming an upward-moving connecting leader. When one of the connecting leaders successfully meets the stepped leader, the thundercloud releases the charges stored inside. In other words, a complete conducting path (channel) is formed, along which a massive current flows towards the ground that makes the channel glow, where a wave of ground potential called the return stroke travels towards the cloud. A single stroke flash is initiated when the lightning flash ends after the first return current stops flowing through the stroke channel (Hazmi et al., 2017).

The features of measurement can be categorised into three different situations. The first situation is when the size of the sensor is tiny compared to the field wavelength across the object; hence, the electric and magnetic at field theory can be adopted, which refer to the quasi-static case with a frequency range of 300 Hz to 1 MHz (Bodewein et al., 2019). The second situation is when the sensor's size is equivalent to the field wavelength, usually applied at microwave frequencies from 1 GHz to 100 GHz (Ohring, 1998); hence, precise analysis is required where no estimation can be used in theory. Lastly, when the sensor's size is bigger than the field wavelength, usually applied at optical frequencies ranging from 100 GHz to 10 THz (Calvo-de la Rosa et al., 2020), only the waveform amplitude is considered. Since this study focuses on the electric field measurement, the quasi-static theory is well applicable to this measurement as the electromagnetic wavelength signal is significantly larger than the size of the sensor.

Power distribution parties require lightning location detection to select a new safe power grid site for system protection. The evaluation of a lightning location is one of the critical issues for lightning mapping and considers the level of lightning risk for power systems protection. Several studies have evaluated lightning locations, usually based on the time of arrival of a measured electric field (Rakov, 2013). The lightning activity produced by thunderstorms can be detected using a lightning detection system (LDS), which can be ground-based, mobile-based as well as space-based (satellite) (Haddad et al., 2012). Meanwhile, a lightning protection system (LPS) works by providing a path of electric discharge to the ground. The LPS can be operated based on the measured and validated data obtained by the LDS. Developing such systems (i.e. LDS and LPS) requires an understanding of the theoretical background of lightning physics, which is related to technical and engineering matters. Apart from the modern and sophisticated equipment

requirement, a proper detection network is also vital in LDS, which is dependent on the characteristics and features of lightning due to its very complex nature/atmospheric phenomenon.

Hence, many studies have been conducted to measure, analyse and characterise the lightning-generated electric field waveform in tropical and non-tropical regions. A tropical climate is characterised by having the lowest month's mean temperature of 18°C or higher. Most tropical locations are well known for having seasons in the monsoon, warm and cool, and wet and dry seasons (Trewin, 2014). Meanwhile, the equatorial region is characterised by consistent warmth (Brohan et al., 2006). Non-tropical regions/countries are also known as temperate countries, which encounter very cold and hot or winter and summer weather due to their location outside the tropics (Tushabe, 2020). Non-tropical regions also experience scorching and cold temperatures since they are far and further away from the equator. Numerous studies have described the lightning electric field's measurement and characteristics in a tropical and non-tropical region (Hazmi et al., 2013; Chi et al., 2014; Quick & Krider, 2014; Wooi et al., 2015; Yusop et al., 2019). This paper presents the feature of negative lightning return strokes in the central region in peninsular Malaysia with a geographical coordinate of (Latitude: 2.973270N, and Longitude: 101.728536E). We also investigate the comparison of the negative lightning return strokes characteristic between tropical and non-tropical regions based on the statistical analysis.

METHODOLOGY

There is a motion of charges generated from lightning across the atmosphere's vicinity in the lightning phenomenon. Based on this movement, the lightning measurement can be carried out either for radiation (fast field), electrostatic (slow field), or induction (magnetic field) (Baharudin et al., 2012). Only the radiation component of the fast field measurement propagated by lightning is highlighted in this study. Figure 1 illustrates the radiation (fast field) measurement setup. Based on Figure 1, the radiation field propagates on the parallel plate antenna when lightning occurs. The radiation field propagation is interpreted as an induced voltage from a certain distance denoted by *d*. The signal measured by the parallel plate antenna is transferred to the transient recorder system via a coaxial cable. A waveform of voltage versus time indicating the electric field change is then interpreted from the recorded signal by the transient recorder system.

The study recorded the lightning-generated electric field waveforms using a parallel-plate antenna from August 2019 to March 2020. This duration covered different seasonal periods in Malaysia, such as the northeast monsoon (December to February), first inter-monsoonal (March to April), southeast monsoon (May to September), and the second inter-monsoonal (October to November). The field test measurement was conducted on the College of Engineering building rooftop at UNITEN. Its proximity to the equator is
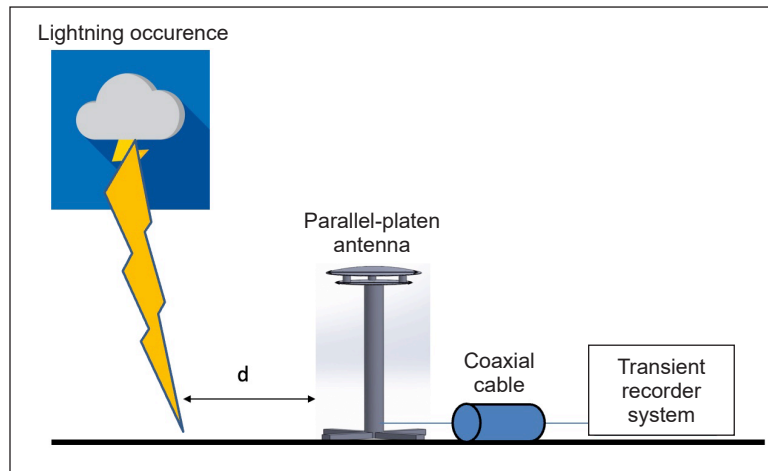
Figure 1. Lightning electric field measurement

given by geographic coordinates of latitude and longitude of 2.973270N and 101.728536E, respectively. The antenna used in this study had a height of 0.555m, a diameter of 0.25 m and a distance between plates of 0.03 m.

A specific electronic circuit was used to measure the electric field waveforms of this study interest for lightning electric field measurement. An electronic buffer circuit has been adopted in this study, widely used in previous studies (Mehranzamir et al., 2019; Rojas et al., 2017; Sonnadara et al., 2006). The electronic buffer circuit was designed mainly on the fast field of electric field measurement, and one of the crucial element was the decay time constant of the whole system. This element is composed of the RC (resistor-capacitor) filter circuit, where the decay time constant should be within a range of 10 ms for fast field and 1s for slow field measurement. Based on the schematic diagram shown in Figure 2, the electronic buffer circuit can be divided into three parts: (1) RC filter, (2) buffer amplifier, and (3) an impedance matching circuit. The RC filter was connected with input from the parallel-plate antenna (Vg), and the filter was composed of R1=50 Ω, R2=100 MΩ, and C=15 pF. The capacitance (C) value in the RC filter circuit was chosen carefully to control the decay time. Accordingly, a capacitance of 15 pF was required to control the decay time constant for fast field measurement.

Meanwhile, for slow field measurement, the required capacitance was 10 nF. Apart from that, the R2 value was as high as 100 MΩ to maintain the decay time constant of fast field measurement since the input impedance was very high. Thus, it was vital to keep the value of C as low as possible to keep the whole system's gain at a reasonable value, meaning that a high C value would result in a low overall gain of the antenna system. The next element of the circuit was the buffer amplifier, an essential component in the electronic buffer circuit. Since the parallel-plate antenna carried high impedance and high output signals, it could cause damage to the transient recorder system. Therefore, the buffer
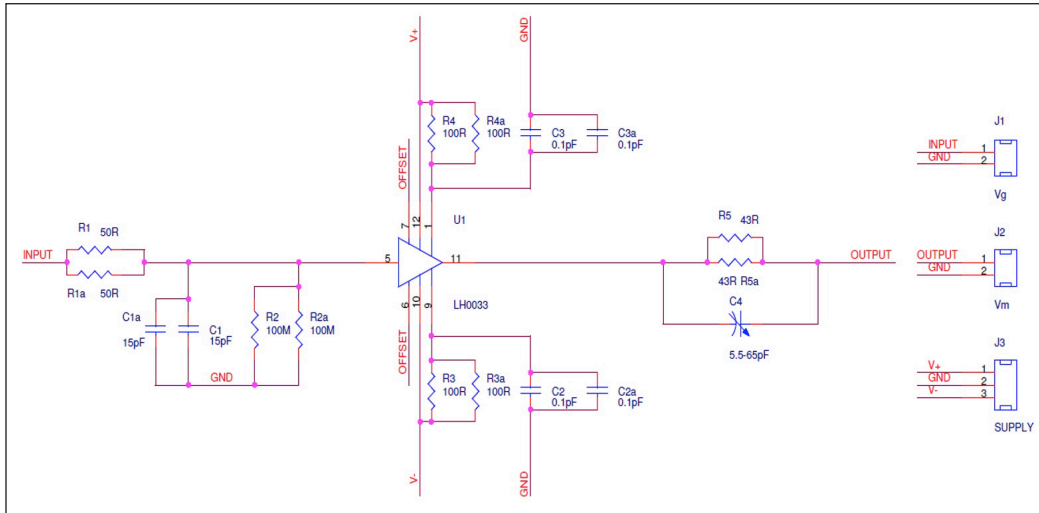
Figure 2. Schematic diagram of buffer amplifier circuit

amplifier was used to isolate the high impedance of the parallel-plate antenna and provide enough power to drive a signal from the antenna input to the transient recorder system through a coaxial cable. This study used the MSK0033 component as the buffer amplifier that offered a high current drive. The high-speed operational amplifier MSK0033 also acted to control the bandwidth of the whole system up to 140 MHz, which was reasonable for a peak frequency range between 10 to 300 kHz.

The transient recorder system used was the PicoScope (PC Oscilloscope) 4000 series. A virtual instrument was formed by connecting the PicoScope oscilloscope to a computer via Picoscope software. This 12-bit oscilloscope comprises BNC (Bayonet Neill–Concelman) type connectors whose inputs have an impedance of 1 MΩ that is compatible with all standard scope probes, including x1, x10, and switched types. In this study, the sampling rate was set to 25 MS/s (Mega samples per second) which was deemed adequate to record the lightning electric field waveforms (Esa et al., 2014). Meanwhile, the total length of recorded waveforms was 200ms per division. Another important setting parameter that plays a significant role in lightning electric field measurement is the triggering level, which consists of the vertical axis (for voltage) and the horizontal axis (for time). For voltage triggering, the edge triggering based on the oscilloscope feature is the widely practised method for capturing edge triggering events, such as the lightning electric field at a specific voltage. The voltage triggering level must be set wisely, where it cannot be overly high or too low. If the triggering level were set too low, the oscilloscope would easily capture an unnecessary and undesirable signal, such as noises. On the other hand, if the triggering threshold value was set overly high, such as 500 mV, the oscilloscope might not capture a generated return stroke of the electric field with an amplitude of 250 mV. Consequently, both conditions might lead to wasted time and opportunity as the actual lightning electric

field events would have been lost or missed to be captured by the oscilloscope. In this study, the set voltage triggering level was 200 mV, while the horizontal axis was 100 ms (for the trigger time).

RESULTS AND DISCUSSIONS

This study recorded 205 lightning signals and successfully identified 115 negative return strokes from the signals. Figures 3(a)–(d) and Figure 4 shows an example of the measured negative return stroke signal with the negative stroke's zooming, in which the signal represents up to the zero-crossings. The negative lightning return stroke characteristic was compared with seven negative return stroke parameters between a tropical and non-tropical region. The parameters involved are zero to peak rise time, 10 to 90% rise time, zero-crossing time, slow front duration, slow front amplitude relative to the peak, fast transition 10 to 90% rise time, and width dE/dt pulse at half peak. In this case, each of the parameters was compared in terms of the range of the data, arithmetic mean (AM), and standard deviation (SD).
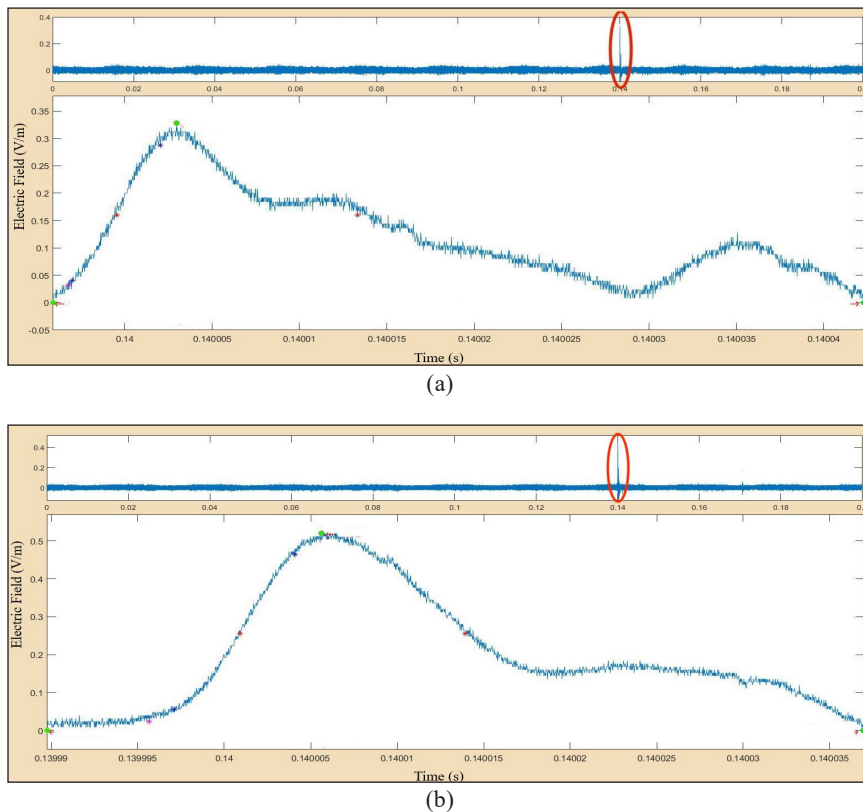

(a)

(b)

Figure 3. (a) Measured negative lightning return strokes; and (b) Measured negative lightning return strokes
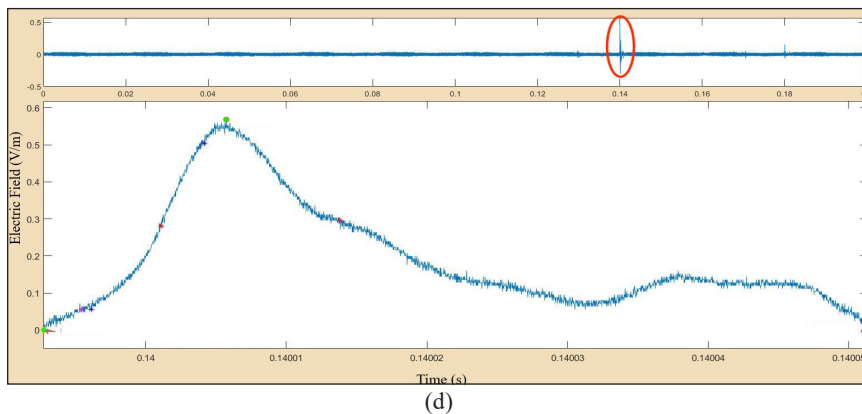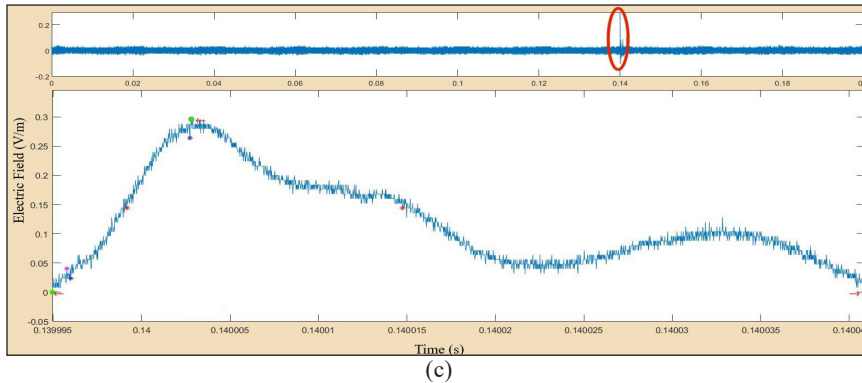
(c)

(d)

Figure 3 (continue). (c) Measured negative lightning return strokes; and (d) Measured negative lightning return strokes
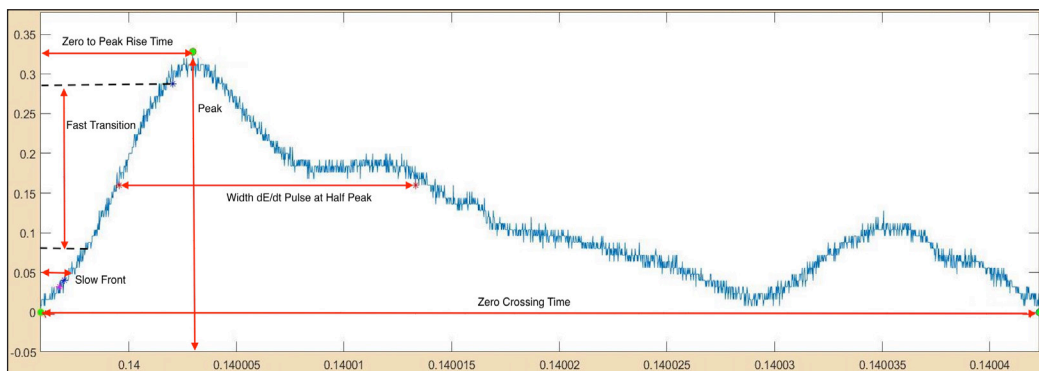

Figure 4. Negative return stroke parameters

Zero to Peak Rise Time

The range of the zero to peak rise of this study was observed within 1.68 µs and 19.72 µs. Figure 5 shows the associated histogram plot, where the highest occurrence was identified within 6 µs to 8 µs. Comparison with the data by Arshad (2017) revealed that the AM

(6.70) and SD (2.57) for this specific parameter of this study were in line, respectively. Additionally, the findings of this study were consistent with the findings by Wooi et al. (2016) (AM = 6.60, SD = 2.9), where the measurement was conducted in southern Malaysia. Based on Table 1, most of the zero to peak rise time measured from the non-tropical region was significantly lower than data measured in a tropical region. Lin et al. (1979) found that the AM and SD for this parameter are 2.4 and 1.2. Meanwhile, the data measured by Fisher and Uman (1972) was observed as 3.7. This finding is consistent with the AM determined by Master and Uman (1984) and Heidler and Hopf (1998), which are 4.4. and 5.3, respectively.
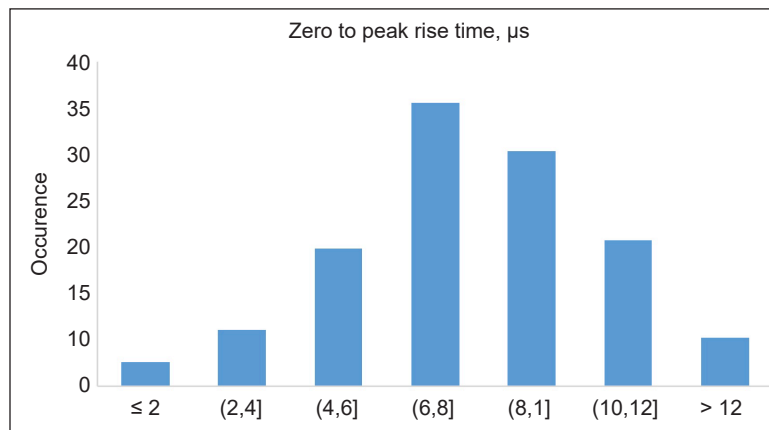

Figure 5. Histogram of zero to peak rise time

Table 1

Summary of zero to peak rise time in a tropical and non-tropical region

Authors	Location	Region	SS	AM	SD
This Study	Uniten,Malaysia	Tropical	115	6.70	2.57
Wooi et al., 2016	UTM, Malaysia	Tropical	104	6.60	2.90
Arshad, 2017	UPM, Malaysia	Tropical	142	6.65	2.68
Fisher and Uman, 1972	Coraopolis, USA	Non-Tropical	436	3.7	-
Lin et al., 1979	KSC, USA	Non-Tropical	51	2.4	1.2
Cooray and Lundquist, 1982	Sweden	Non-Tropical	140	7	2
Master et al., 1984	Florida, USA	Non-Tropical	105	4.4	1.8
Heidler et al., 1998	Germany	Non-Tropical	148	5.3	3.2

Note. SS: Sample size; AM: Arithmetic mean; SD: Standard deviation

10-to-90% Rise Time

The range of the 10 to 90% rise time for this study was observed from 3.7 to 8.90 µs, considered in line with the data measured in (Arshad, 2017), which was observed from 0.54 µs and 9.32 µs. Figure 6 shows the associated histogram plot, where the highest occurrence

was identified as less than 4 µs. Comparison with the data in (Arshad, 2017) (AM = 4.30, SD = 1.73) revealed that the AM (4.51) and SD (1.25) for the particular parameter of this study were consistent, respectively. This observation was also in line with the data measured by Wooi et al. (2016) (AM = 3.9, SD = 2.6). Meanwhile, the calculated AM for the 10 to 90% rise time of non-tropical region (Hojo et al., 1985) was observed consistent with this study (AM = 3.9), as shown in Table 2. However, the data reported by Master and Uman (1984) was observed slightly lower as compared to the others with AM of 2.6.
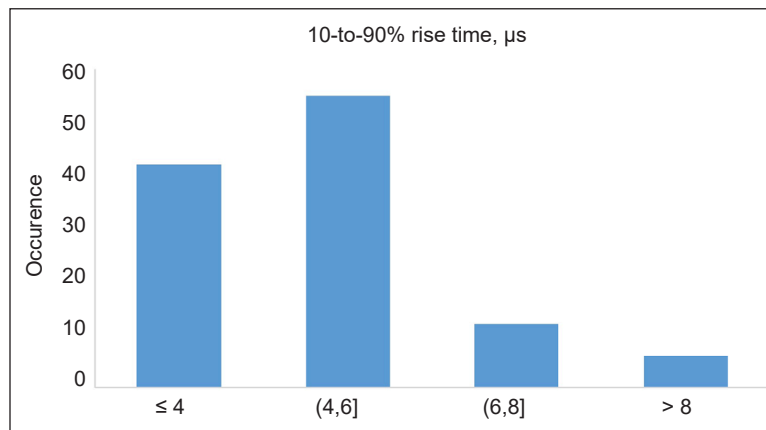

Figure 6. Histogram of 10-to-90% rise time

Table 2
Summary of 10-to-90% rise time in a tropical and non-tropical region

Authors	Location	Region	SS	AM	SD
This Study	Uniten, Malaysia	Tropical	115	4.51	1.25
Wooi et al., 2016	UTM, Malaysia	Tropical	104	3.9	2.6
Arshad, 2017	UPM, Malaysia	Tropical	142	4.03	1.73
Willett and Krider, 2000	Florida, USA	Non-Tropical	76	-	-
Hojo et al., 1985	Japan	Non-Tropical	8	3.9	-
Master et al., 1984	Florida, USA	Non-Tropical	105	2.6	1.2

Note. SS: Sample size; AM: Arithmetic mean; SD: Standard deviation

Zero-Crossing Time

Apart from that, the range of the zero-crossing time for this study was observed from 4.69 to 82.52 µs, whereas it was from 4.66 to 82.06 µs for Arshad (2017). Figure 7 shows the associated histogram plot, where the highest occurrence was observed within 30 and 50 µs. The calculated AM was 33.79, slightly higher than Arshad (2017). On the same note, Wooi et al. (2016) reported a much higher AM value (50.7) than this study. On the other hand, the calculated SD for this specific parameter of this study was 12.77, which was slightly lower than Arshad (2017). Also, the data reported in Wooi et al. (2016) is consistent with

the data measured in the same region, Colombia, with AM of 62 (Santamaría et al., 2006). From Table 3, the zero-crossing time reported from Florida, USA (Haddad et al., 2012) in the non-tropical region were significantly longer than the other region with an arithmetic mean of 89. Meanwhile, Heidler and Hopf (1998) recorded the lowest zero-crossing time with arithmetic mean and standard deviation of 5.3 and 3.2, respectively.
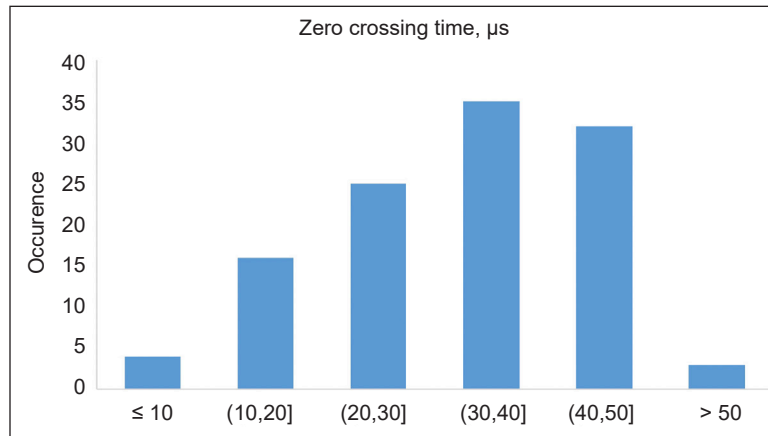

Figure 7. Histogram of zero crossing time

Table 3
Summary of zero crossing time in a tropical and non-tropical region

Authors	Location	Region	SS	AM	SD
This Study	Uniten,Malaysia	Tropical	115	33.79	12.77
Wooi et al., 2016	UTM, Malaysia	Tropical	104	50.7	44.4
Arshad, 2017	UPM, Malaysia	Tropical	142	32.9	13.3
Santamaria et al., 2006	Colombia	Tropical	68	62	-
Haddad et al., 2012	Florida, USA	Non-Tropical	265	89	-
Cooray and Lundquist, 1982	Sweden	Non-Tropical	140	49	12
Heidler et al., 1998	Germany	Non-Tropical	148	5.3	3.2

Note. SS: Sample size; AM: Arithmetic mean; SD: Standard deviation

Slow Front Time

The slow front duration for this study was observed from 0.606 to 9.18 µs, whereas it was from 0.30 to 9.92 µs for Arshad (2017). Figure 8 shows the associated histogram plot, where the highest occurrence was observed within 2 and 4 µs. Comparison with the data in Arshad (2017) (AM = 4.5, SD = 2.6) revealed that the AM (4.36) and SD (2.08) for this specific parameter of this study were consistent, respectively. In addition, these values were observed to be close to the data measured by Wooi et al. (2016) (AM = 4.5, SD = 2.4). From Table 4, the finding of this study was also consistent with the data reported in Sri Lanka (Cooray & Lundquist, 1985) (AM = 4.6, SD = 1.5). The arithmetic mean and

standard deviation measured from Florida and Germany (Heidler & Hopf, 1998; Haddad et al., 2012; Weidman & Krider, 1978) in the non-tropical region was observed in line with all studies conducted in a tropical region. However, the data reported by Cooray and Lundquist (1982) in Sweden was observed slightly lower with AM of 2.9.
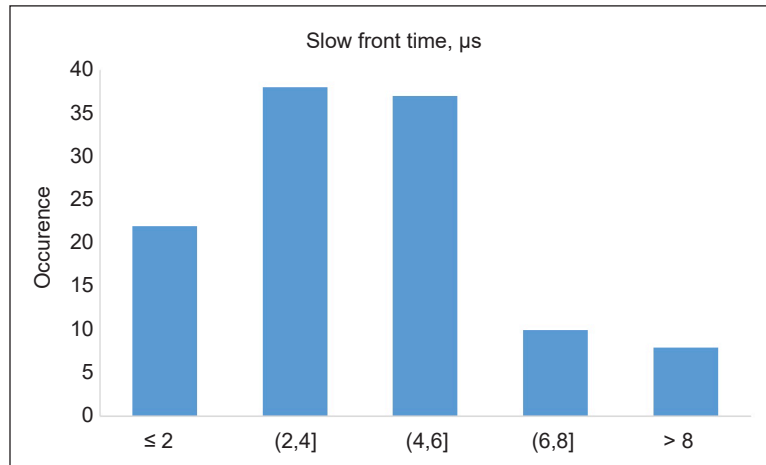

Figure 8. Histogram of slow front time

Table 4
Summary of slow front time in a tropical and non-tropical region

Authors	Location	Region	SS	AM	SD
This Study	Uniten,Malaysia	Tropical	115	4.36	2.08
Wooi et al., 2016	UTM, Malaysia	Tropical	104	4.5	2.4
Arshad, 2017	UPM, Malaysia	Tropical	142	4.5	2.6
Cooray and Lundquist, 1985	Sri Lanka	Tropical	104	4.6	1.5
Haddad et al., 2012	Florida, USA	Non-Tropical	265	5	2
Cooray and Lundquist, 1982	Sweden	Non-Tropical	140	2.9	1.3
Weidman and Krider, 1978	Florida, USA	Non-Tropical	104	4.6	1.5
Heidler et al., 1998	Germany	Non-Tropical	148	4.5	2.4

Note. SS: Sample size; AM: Arithmetic mean; SD: Standard deviation

Slow Front Amplitude Relative to Peak

In this study, the range of the slow front amplitude relative to peak parameter was observed from 7.5% to 43.2%, whereas it was from 0.98% to 78.76% for Arshad (2017). As shown in Figure 9, the highest occurrence for this parameter was observed within 20% to 30%. For this parameter, the arithmetic mean and the standard deviation was calculated as 28.8 and 8.46; meanwhile, the data recorded by Arshad (2017) was determined as 34.4 and 17, respectively. The data recorded from this study is also consistent with those obtained by Wooi et al. (2016) under the same region as illustrated in Table 5. However, the non-tropical

area data was observed significantly higher, such as in KSC, Florida USA, and Sweden with AM and SD ranging from 41–50 and 10–11, respectively (Cooray & Lundquist, 1982; Master & Uman, 1984; Weidman & Krider, 1978; Weidman & Krider, 1980).
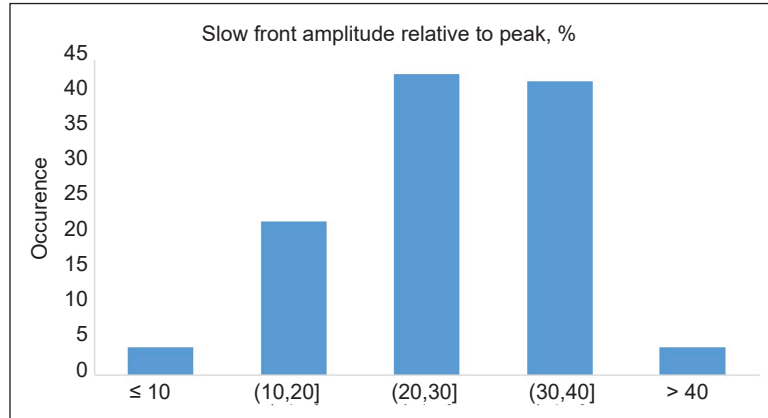

Figure 9. Histogram of slow front amplitude relative to peak

Table 5
Summary of slow front amplitude relative to peak in a tropical and non-tropical region

Authors	Location	Region	SS	AM	SD
This Study	Uniten, Malaysia	Tropical	115	28.8	8.46
Wooi et al., 2016	UTM, Malaysia	Tropical	104	30.8	16.2
Arshad, 2017	UPM, Malaysia	Tropical	142	34.4	17.0
Willett and Krider, 2000	KSC, USA	Non-Tropical	76	50	10
Weidman and Krider, 1978	Florida, USA	Non-Tropical	62	50	-
Cooray and Lundquist, 1982	Sweden	Non-Tropical	140	41	11

Note. SS: Sample size; AM: Arithmetic mean; SD: Standard deviation

Fast Transition 10-to-90% Rise Time

This study's measured data of fast transition 10 to 90% rise time ranged from 2.8 to 10.18 µs, in line with the data in Arshad (2017), which varied from 0.10 µs to 11.32 µs. Based on the associated histogram plot from Figure 10, the highest frequency was observed within 2 and 4 µs. The arithmetic mean was calculated as 3.95, slightly higher than the data recorded from Arshad (2017). On the same note, Wooi et al. (2016) reported a much lower AM value (AM = 1.5) compared to this study. Meanwhile, the calculated SD (1.71) for this specific parameter of this study was slightly higher than Arshad (2017). It is noticeable from Table 6 that the AM and SD for this parameter measured in non-tropical regions were observed significantly lower than the data obtained in tropical regions (Hojo et al., 1985; Master & Uman, 1984; Weidman & Krider, 1978; Weidman & Krider, 1980). Both AM and SD were determined within 0.09 to 0.97 and 0.04 to 0.68, respectively.
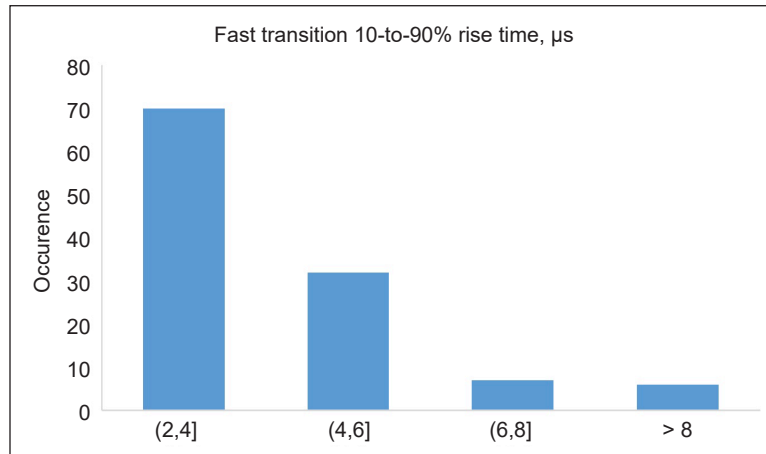
Figure 10. Histogram of fast transition 10-to-90% rise time

Table 6

Summary of fast transition 10-to-90% rise time in a tropical and non-tropical region

Authors	Location	Region	SS	AM	SD
This Study	Uniten, Malaysia	Tropical	115	3.95	1.71
Wooi et al., 2016	UTM, Malaysia	Tropical	104	1.5	1.0
Arshad, 2017	UPM, Malaysia	Tropical	142	2.14	1.65
Weidman and Krider, 1978	Florida, USA	Non-Tropical	125	0.09	0.04
Weidman and Krider, 1980	Florida, USA	Non-Tropical	38	0.2	-
Master et al., 1984	Florida, USA	Non-Tropical	105	0.97	0.68
Hojo et al., 1985	Japan	Non-Tropical	8	0.14	-

Note. SS: Sample size; AM: Arithmetic mean; SD: Standard deviation

Width dE/dt Pulse at Half Peak Value

Furthermore, the range of the width dE/dt pulse at half peak measured from this study was observed from 1.4 to 6.9 µs, whereas it was from 0.56 to 7.48 µs for Arshad (2017). Figure 11 shows the associated histogram plot, where the highest occurrence was identified within 2 to 3 µs. Comparison with the data in Arshad (2017) (AM = 2.7, SD = 1.5) revealed that the AM (3.57) and SD (1.23) for this specific parameter of this study were consistent, respectively. This observation was also in line with the data measured in Wooi et al. (2016) (AM = 2.4, SD = 1.3). However, there was a significant difference in AM and SD reported from the non-tropical region, as shown in Table 7. This data was identified much lower with AM and SD of 0.1 to 0.77 and 0.2 to 0.3 than the data obtained in a tropical region (Heidler & Hopf, 1998; Krider et al., 1996; Willett & Krider, 2000).
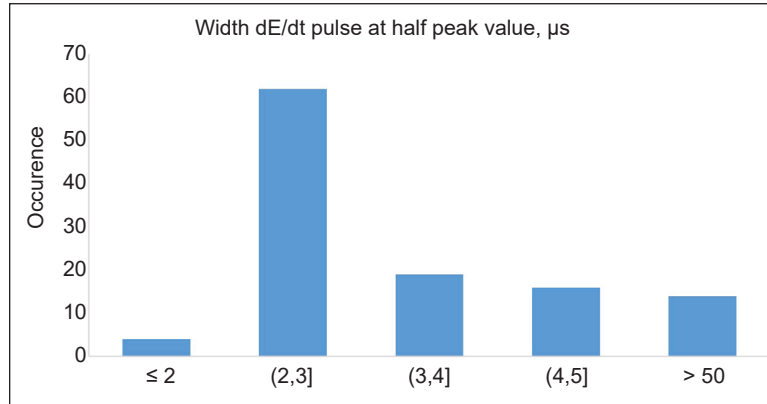
Figure 11. Histogram of width dE/dt pulse at half peak

Table 7
Summary of width dE/dt pulse at half peak value in a tropical and non-tropical region

Authors	Location	Region	SS	AM	SD
This Study	Uniten, Malaysia	Tropical	115	3.57	1.23
Wooi et al., 2016	UTM, Malaysia	Tropical	104	2.4	1.3
Arshad, 2017	UPM, Malaysia	Tropical	142	2.7	1.5
Willett and Krider, 2000	KSC, USA	Non-Tropical	76	0.77	0.2
Krider et al., 1996	Florida, USA	Non-Tropical	61	0.1	0.2
Willet and Krider, 2000	Florida, USA	Non-Tropical	131	0.64	0.22
Heidler et al., 1998	Germany	Non-Tropical	148	0.62	0.3

Note. SS: Sample size; AM: Arithmetic mean; SD: Standard deviation

CONCLUSIONS

This paper presents characteristics of negative lightning return strokes recorded in the central part of peninsular Malaysia, close to the equatorial line. A total of 115 lightning-generated electric fields have been measured and analysed based on the seven types of negative lightning return stroke parameters. In addition, a comparison was made between the data measured in the tropical and non-tropical regions in terms of the characteristic mainly on the negative return strokes parameters, such as zero-to-peak rise time, 10 to 90% rise time, zero-crossing time, slow front duration, slow front amplitude relative to the peak, fast transition 10 to 90% rise time, and width dE/dt pulse at half peak value. In this study, statistical data at various countries in a tropical region have been compared, such as Malaysia, Colombo, and Sri Lanka. Meanwhile, the non-tropical region involved several countries, including Sweden, Germany, Japan, and the USA. From the results, it can be seen that most of the arithmetic mean and standard deviation of each parameter shows a good agreement with the data measured from the same region. In this case, the recorded data

from this study does not differ much from the measured data in the same region reported by Arshad (2017). On the same note, the findings of this study were consistent with the previous study conducted at the University Teknologi Malaysia (UTM) in the southern part of Malaysia (Wooi et al., 2016).

Compared to the non-tropical region, the data also match with 10 to 90% rise time and slow front time parameters. Nevertheless, there was a significant difference between these two regions in the zero to peak rise time parameter. Based on the statistical data in the non-tropical region, the AM and SD were observed (20.90% to 64.18%) and (24.5% to 53.3%) lower than a tropical data measurement. Meanwhile, most of the zero-crossing time in the non-tropical region was identified significantly longer than a tropical region with a percentage difference of 41.3% to 62%. Similar to slow front amplitude relative to the peak, it was observed 30% to 42.4% higher than the tropical region's data. Furthermore, a considerable difference was observed between a tropical and non-tropical region in fast transition 10 to 90% rise time and width dE/dt pulse at half peak. In this part, the AM and SD of fast transition 10 to 90% rise time measured in a tropical region were discovered 75.4% to 96% and 60.23% to 97.66% higher than those obtained from a non-tropical region. This finding is consistent with the width dE/dt pulse at half peak parameter. Both AM and SD reported in a tropical region were observed significantly higher than a non-tropical region with a percentage difference of 78.43% to 82.63% and 75.61% to 83.74%. A significant difference in the data comparison with different countries, mainly from the non-tropical region, was observed due to geographical locations, meteorological conditions, and climatic variations. It was likely because most tropical areas near the equator are not affected by or experiencing the seasonal variations of non-tropical areas, specifically spring, summer, fall, and winter.

ACKNOWLEDGEMENTS

REFERENCES

Ahmad, N. A., Fernando, M., Baharudin, Z. A., Cooray, V., Ahmad, H., & Malek, Z. A. (2010). Characteristics of narrow bipolar pulses observed in Malaysia. *Journal of Atmospheric and Solar-Terrestrial Physics, 72*(5-6), 534-540. https://doi.org/10.1016/j.jastp.2010.02.006

Arshad, S. A. M. (2017). *Characterization of lightning-generated electric fields and development of automated measuring system for cloud-to-ground lightning in Malaysia* (Doctoral dissertation). Universiti Putra Malaysia. http://psasir.upm.edu.my/id/eprint/70239.

Baharudin, Z. A., Fernando, M., Ahmad, N. A., Mäkelä, J. S., Rahman, M., & Cooray, V. (2012). Electric field changes generated by the preliminary breakdown for the negative cloud-to-ground lightning flashes in Malaysia and Sweden. *Journal of Atmospheric and Solar-Terrestrial Physics, 84*, 15-24. https://doi.org/10.1016/j.jastp.2012.04.009

Bodewein, L., Schmiedchen, K., Dechent, D., Stunder, D., Graefrath, D., Winter, L., Kraus, T., & Driessen, S. (2019). Systematic review on the biological effects of electric, magnetic and electromagnetic fields in the intermediate frequency range (300 Hz to 1 MHz). *Environmental Research, 171*, 247-259. https://doi.org/10.1016/j.envres.2019.01.015

Brohan, P., Kennedy, J. J., Harris, I., Tett, S. F. B., & Jones, P. D. (2006). Uncertainty estimates in regional and global observed temperature changes: A new data set from 1850. *Journal of Geophysical Research Atmospheres, 111*(D12), 1-21. https://doi.org/10.1029/2005JD006548

Calvo-de la Rosa, J., Locquet, A., Bouscaud, D., Berveiller, S., & Citrin, D. S. (2020). Optical constants of CuO and ZnO particles in the terahertz frequency range. *Ceramics International, 46*(15), 24110-24119. https://doi.org/10.1016/j.ceramint.2020.06.190

Chi, G., Zhang, Y., Zheng, D., Lu, W., & Zhang, Y. (2014). Characteristics of lightning activities in Potala Palace region of Tibet. In *2014 International Conference on Lightning Protection (ICLP)* (pp. 1992-1994). IEEE Publishing. https://doi.org/10.1109/ICLP.2014.6973455

Cooray, V., & Lundquist, S. (1985). Characteristics of the radiation fields from lightning in Sri Lanka in the tropics. *Journal of Geophysical Research, 90*(D4), 6099-6109. https://doi.org/10.1029/JD090iD04p06099

Cooray, V. (1997). A model for negative first return strokes in lightning flashes. *Physica Scripta, 55*(1), Article 119. https://doi.org/10.1088/0031-8949/55/1/024

Cooray, V. (2015). Charge generation in thunderclouds and different forms of lightning flashes. In *An Introduction to Lightning* (pp. 79-89). Springer. https://doi.org/10.1007/978-94-017-8938-7_6

Cooray, V., & Fernando, M. (2009). Lightning parameters of engineering interest. In V. Cooray (Ed.), *Lightning Protection* (pp. 15-96). The Institution of Engineering and Technology. https://doi.org/10.1049/PBPO058E_ch2

Cooray, V., & Lundquist, S. (1982). On the characteristics of some radiation fields from lightning and their possible origin in positive ground flashes. *Journal of Geophysical Research, 87*(C13), 11203-11214. https://doi.org/10.1029/jc087ic13p11203

Dwyer, J. R., & Uman, M. A. (2014). The physics of lightning. *Physics Reports, 534*(4), 147-241. https://doi.org/10.1016/j.physrep.2013.09.004

Esa, M. R. M., Ahmad, M. R., Cooray, V., & Esa, M. R. M. (2014). Occurrence of narrow bipolar pulses between negative return strokes in tropical thunderstorms. In *2014 International Conference on Lightning Protection (ICLP)* (pp. 1141-1142). IEEE Publishing. https://doi.org/10.1109/ICLP.2014.6973297

Fisher, R. J., & Uman, M. A. (1972). Measured electric field risetimes for first and subsequent lightning return strokes. *Journal of Geophysical Research, 77*(3), 399-406. https://doi.org/10.1029/jc077i003p00399

Haddad, M. A., Rakov, V. A., & Cummer, S. A. (2012). New measurements of lightning electric fields in Florida: Waveform characteristics, interaction with the ionosphere, and peak current estimates. *Journal of Geophysical Research Atmospheres, 117*(D10), 1-26. https://doi.org/10.1029/2011JD017196

Hazmi, A., Emeraldi, P., Hamid, M. I., & Takagi, N. (2017). Research on positive narrow bipolar events in Padang. In *2016 3rd International Conference on Information Technology, Computer, and Electrical Engineering (ICITACEE)* (pp. 156-159). IEEE Publishing. https://doi.org/10.1109/ICITACEE.2016.7892429

Hazmi, A., Hendri, Z., Mulyadi, S., Tesal, D., Wang, D., & Takagi, N. (2013). Characteristics of electric field change preceding negative first return stroke produced by preliminary breakdown. In *2013 International Conference on Information Technology and Electrical Engineering (ICITEE)* (pp. 322-325). IEEE Publishing. https://doi.org/10.1109/ICITEED.2013.6676261

Heidler, F., & Hopf, C. (1998). Measurement results of the electric fields in cloud-to-ground lightning in nearby Munich, Germany. *IEEE Transactions on Electromagnetic Compatibility, 40*(4), 436-443. https://doi.org/10.1109/15.736204

Hojo, J., Ishii, M., Kawamura, T., Suzuki, F., & Funayama, R. (1985). The fine structure in the field change produced by positive ground strokes. *Journal of Geophysical Research, 90*(D4), 6139-6143. https://doi.org/10.1029/JD090iD04p06139

Krider, E. P., Leteinturier, C., & Willett, J. C. (1996). Submicrosecond fields radiated during the onset of first return strokes in cloud-to-ground lightning. *Journal of Geophysical Research Atmospheres*, *101*(D1), 1589-1597. https://doi.org/10.1029/95JD02998

Lin, Y. T., Uman, M. A., Tiller, J. A., Brantley, R. D., Beasley, W. H., Krider, E. P., & Weidman, C. D. (1979). Characterization of lightning return stroke electric and magnetic fields from simultaneous two-station measurements. *Journal of Geophysical Research, 84*(C10), 6307-6314. https://doi.org/10.1029/JC084iC10p06307

Master, M. J., & Uman, M. A. (1984). Lightning induced voltages on power lines: Theory. *IEEE Transactions on Power Apparatus and Systems, PAS-103*(9), 2502-2518. https://doi.org/10.1109/TPAS.1984.318405

Mehranzamir, K., Afrouzi, H. N., Abdul-Malek, Z., Nawawi, Z., Sidik, M. A. B., & Jambak, M. I. (2019). Hardware installation of lightning locating system using time difference of arrival method. In *2019 International Conference on Electrical Engineering and Computer Science (ICECOS)* (pp. 29-34). IEEE Publishing. https://doi.org/10.1109/ICECOS47637.2019.8984497

Nag, A., & Rakov, V. A. (2014). Parameters of electric field waveforms produced by positive lightning return strokes. *IEEE Transactions on Electromagnetic Compatibility, 56*(4), 932-939. https://doi.org/10.1109/TEMC.2013.2293628

Ohring, M. (1998). Electronic devices: How they operate and are fabricated. In *Reliability and Failure of Electronic Materials and Devices* (pp. 37-105). Academic Press. https://doi.org/10.1016/b978-012524985-0/50003-9

Quick, M. G., & Krider, E. P. (2014). Optical emission and peak electromagnetic power radiated by return strokes in rocket-triggered lightning. In *2014 International Conference on Lightning Protection (ICLP)* (pp. 2011-2015). IEEE Publishing. https://doi.org/10.1109/ICLP.2014.6973459

Rakov, V. A. (2013). The physics of lightning. *Surveys in Geophysics, 34*(6), 701-729. https://doi.org/10.1007/s10712-013-9230-6

Rakov, V. A., & Uman, M. A. (2003). *Lightning: Physics and effects.* Cambridge University Press. https://doi.org/10.1256/wea.168/03

Rojas, H., Cruz, A., & Cortés, C. (2017). Characteristics of lightning-generated electric fields measured in the Bogotá Savanna, Colombia. *Revista UIS Ingenierías, 16*(2), 243-252. https://doi.org/10.18273/revuin.v16n2-2017022

Santamaría, F., Gomes, C., & Roman, F. (2006, September 18-22). Comparison between the signatures of lightning electric field measured in Colombia and that in Sri Lanka. In *Proceedings of the 28th International Conference on Lightning Protection* (pp. 254-256), Kanazawa, Japan. https://doi.org/10.14936/ieiej.27.226

Shivalli, S. (2016). Lightning phenomenon, effects and protection of structures from lightning. *IOSR Journal of Electrical and Electronics Engineering (IOSR-JEEE), 11*, 44-50. https://doi.org/10.9790/1676-1103014450

Sokol, Z., & Popová, J. (2021). Differences in cloud radar phase and power in co-and cross-channel-indicator of lightning. *Remote Sensing, 13*(3), Article 503. https://doi.org/10.3390/rs13030503

Sonnadara, U., Cooray, V., & Fernando, M. (2006). The lightning radiation field spectra of cloud flashes in the interval from 20 kHz to 20 MHz. *IEEE Transactions on Electromagnetic Compatibility, 48*(1), 234-239. https://doi.org/10.1109/TEMC.2006.870692

Trewin, B. (Ed.). (2014). *The climates of the Tropics, and how they are changing.* Academic Press.

Tushabe, F. (2020). Comparison of COVID-19 severity between tropical and non-tropical countries. *International Journal of Infection, 7*(3), e104142. https://doi.org/10.5812/iji.104142

Wang, Y., Lu, G., Shi, T., Ma, M., Zhu, B., Liu, D., Peng, C., & Wang, Y. (2021). Enhancement of cloud-to-ground lightning activity caused by the urban effect: A case study in the beijing metropolitan area. *Remote Sensing, 13*(7), Article 1228. https://doi.org/10.3390/rs13071228

Weidman, C. D., & Krider, E. P. (1978). The fine structure of lightning return stroke wave forms. *Journal of Geophysical Research, 83*(C12), 6239-6247. https://doi.org/10.1029/jc083ic12p06239

Weidman, C. D., & Krider, E. P. (1980). Submicrosecond risetimes in lightning return-stroke fields. *Geophysical Research Letters*, *7*(11), 955-958. https://doi.org/10.1029/GL007i011p00955

Willett, J. C., & Krider, E. P. (2000). Rise times of impulsive high-current processes in cloud-to-ground lightning. *IEEE Transactions on Antennas and Propagation, 48*(9), 1442-1451. https://doi.org/10.1109/8.898779

Wooi, C. L., Abdul-Malek, Z., Ahmad, N. A., & El Gayar, A. I. (2016). Statistical analysis of electric field parameters for negative lightning in Malaysia. *Journal of Atmospheric and Solar-Terrestrial Physics, 146*, 69-80. https://doi.org/10.1016/j.jastp.2016.05.007

Wooi, C. L., Abdul-Malek, Z., Ahmad, N. A., & Mokhtari, M. (2015). Characteristic of preliminary breakdown preceding negative return stroke in Malaysia. In *2015 IEEE Conference on Energy Conversion (CENCON)* (pp. 112-115). IEEE Publishing. https://doi.org/10.1109/CENCON.2015.7409523

Yusop, N., Ahmad, M. R., Abdullah, M., Zainudin, S. K., Nor, W. N. A. W. M., Alhasa, K. M., Esa, M. R. M., Sabri, M. H. M., Suparta, W., Gulisano, A. M., & Cooray, V. (2019). Cloud-to-Ground lightning observations over the Western Antarctic region. *Polar Science, 20*, 84-91. https://doi.org/10.1016/j.polar.2019.05.002